Vol. 20, No. 1 (2021) 1-11
Revista Mexicana de Ingeniería Química

Characterization of slug flow in heavy oil and gas mixtures

Caracterización del flujo *slug* en mezclas de aceite pesado y gas

C.A. Carcaño-Silvan[1], G. Soto-Cortes[2], F. Rivera-Trejo[1]*

[1] *Universidad Juárez Autónoma de Tabasco. División Académica de Ingeniería y Arquitectura, carretera Cunduacán-Jalpa KM. 1 Col. La Esmeralda CP. 86690.*
[2] *Universidad Autónoma Metropolitana, Unidad Lerma. Av. de las Garzas No. 10, Col. El Panteón, municipio Lerma de Villada, Estado de México, C.P. 52005.*

Received: February 6, 2020; Accepted: March 26, 2020

Abstract

In multiphase flow, one of the most recurring flow patterns is called slug. Its characterization is essential to predict the drop pressure and liquid holdup. To analyze it, an option is to use a capacitive or inductive sensor to transform the liquid-gas fraction present in the pipeline to a voltage time-series. The method chosen for the signal processing is decisive for the correct estimation of the frequency and the fraction of the slug, among other parameters. Recently, analysis methodologies have been developed that reduce the subjectivity of signal processing and tend to improve the quality of the results. This paper applied an algorithm optimization based on probabilistic methods. The methodology proposed was compared against the original, finding that with the optimization, there is the better performance when working at inclination angles close to the vertical; the above suggests a combined use of both methods.

Keywords: oil-gas flow, slug patter, signal processing, ascending flow, holdup.

Resumen

En los flujos multifásicos uno de los patrones de flujo más recurrente es el llamado slug. Su caracterización es fundamental para predecir la caída de presión y el colgamiento líquido. Para analizarlo, una opción son los sensores capacitivos o inductivos que transforman la fracción liquido-gas presente en la tubería a una serie de tiempo de voltaje. El método elegido para el procesamiento de la señal es determinante para la correcta estimación de la frecuencia, y la fracción del slug entre otros parámetros. Recientemente, se han desarrollado metodologías de análisis que reducen la subjetividad del procesamiento de la señal, y que tienden a mejorar la calidad de los resultados. Este trabajo aplicó una optimización a un algoritmo basado en métodos probabilísticos. Se comparó la metodología propuesta contra la original encontrando que con la optimización se tiene un mejor desempeño cuando se trabaja en ángulos de inclinación cercanos a la vertical. Lo anterior sugiere un uso combinado del método original y la optimización propuesta.

Palabras clave: Flujo aceite-gas, flujo slug, procesamiento de señales, flujo ascendente, colgamiento líquido.

1 Introduction

The processes engineering designs, implements, and executes all the operations necessary to transport, transform, or obtain several products, so it is present in all controls of industrial activity. Many of the industrial processes involve the transport of fluids in one or more phases (Salazar-Mendoza *et al*., 2004; Álvarez del Castillo *et al*., 2010). The difficulty in the design and operation of multiphase flow systems increases as a function of the number of the present phases (Shoham, 2005). The current challenge in the field of multiphase flow lies in the identification and prediction of the geometric arrangement between phases during the transport process. The geometrical arrangement is named flow pattern. Similarly, as hydraulic studies in one phase, in the study of multiphase flow, the flow pattern is the fundamental condition for understanding its relationship to other flow variables such as pressure and energy gradients. Therefore, it is essential to determine the flow pattern for the design, operation, and optimization of multiphase transport systems.

* *Corresponding author. E-mail*: jgfabianrivera@gmail.com
https://doi.org/10.24275/rmiq/Proc1289
issn-e: 2395-8472

The case of liquid-gas mixtures represents an important area of scientific interest due to its predominance in various industrial processes; for example, food, power generation, aeronautics, and petrochemicals, among others (Shoham, 2005). About the oil industry, the prediction and identification of flow patterns - geometric arrangements - between different phases, has been the object of study since the mid-twentieth century (Gfeller and Bapst, 1979; Gregory *et al*., 1978; Taitel and Dukler, 1977). The correct identification and prediction of the flow pattern help the design of transport and distribution systems of oils and gas.

Within the classification of liquid-gas flow patterns, the slug type occurs most frequently, so its study is broad (Al-Ruhaimani *et al*., 2018; Archibong-Eso *et al*., 2018; Baba *et al*., 2017a; F. Sánchez-Silva *et al*., 2018; Zhang *et al*., 2018). One of the main characteristics of the slug flow is the presence of large gas bubbles that separate the liquid column in sections. These bubbles are known as Taylor bubbles (Davies and Taylor, 1950), and they are bullet-shaped - a rounded front shape with a cylindrical body - wrapped in a thin layer of liquid called film. Figure 1 (a) described its components: film length (L_F), liquid slug length (L_S), slug cycle length (L_U), the thickness of the liquid film that covers the bubble (h_F) and its translational velocity (v_T). The holdup is represented as H_{LS} and H_{LF} for the liquid holdup and the liquid film, respectively. The slug flow hydrodynamic characterization is challenging because it involves an unsteady flow-behavior. In addition to the translational velocity v_T, which represents the interface velocity in the main flow direction, a set of secondary velocities must be considered along with the slug unit. Within the slug body the liquid and gas phase velocity in the same direction of v_T are represented by v_{LB} and v_{GB}. In the film (stratified) region the liquid-film velocity v_{LF} and the gas-pocket velocity v_{GF} runs in the opposite direction. According to Taitel and Barnea (1990), the velocity distribution is $v_T > v_{GF} > v_{GB} > v_{LB} > v_{LF}$.

Most of the experimental works related to the slug flow reported in the literature were performed with low viscosity oils (<20 mPa s). However, due to the worldwide reduction of light oil reserves (Alboudwarej *et al*., 2006), research on oils with high and very high viscosity (between 100 and 1000 mPa s) has been intensified. For example, Wu *et al*., (2017) conducted an extensive review of the leading experimental techniques for the identification of flow patterns, as well as the existing models for predicting transitions between them. They classified the experimental methods as visual and non-visual. The visual employ high-speed video cameras (Al-Kayiem *et al*., 2017; Thaker and Banerjee, 2015, 2016) and electrical capacitance tomography (Baba *et al*., 2017b). Non-visual, use gamma-ray induction (Baba *et al*., 2018), and capacitive filament sensors (Al-Ruhaimani, 2015; Brito, Pereyra, & Sarica, 2014; Chung *et al*., 2016). The capacitive sensors are instruments that respond effectively to the variations of liquid and gas present in the mixture over a series of voltage times, whose characteristics are closely related to the present flow pattern. In the present study, we used a database obtained from capacitive sensors.

In Figure 1(a), the slug and film regions are highlighted. Figure 1 (b) presents an example of the data generated through capacitive sensors, with a normalized voltage time series (dimensionless), V' with an acquisition frequency of 1000 Hz. Figure 1 (c) extends the green frame shown in Figure 1(b), corresponding to 2 seconds of experimentation. The relationship between translational velocity, slug, film, and slug cycle lengths are schematized for the time intervals of Δt_S, Δt_F, and Δt_U. Where Δt_S (s) and Δt_F (s) are the ratios of the translational velocity between the length of the liquid slug and the length of the film, respectively, and Δt_U (s) corresponds to the sum of the variables Δt_S and Δt_F.

The challenge in the characterization of the slug flow through a time series − as described in Figure 1 (b) − has three stages. The first one determines the geometric and physical variables as a function of the time; in the second, develops models to describe the relationship between these variables and conservation laws; and finally, these models are used to infer other flow conditions.

As can be anticipated the first stage conditions subsequent ones, and has a decisive role in the characterization of the slug flow (Al-Ruhaimani *et al*., 2018; Al-safran, 2003; Al-Safran, 2016; Gonçalves *et al*., 2018; Jaeger *et al*., 2018; Losi *et al*., 2016; Saidj *et al*., 2018). Therefore, this research focused on the determination of geometric and physical variables. It translates into determining throughout the time series, objectively and consistently, the beginning and end of the Taylor bubble; however, there is currently no standardized methodology to achieve it.

Kouba (1986) presented one of the first studies for signal processing generated by capacitive sensors. They transformed the normalized voltage time series V' (Figure 1 (b)), from a visually selected cut-off threshold (THV, Figure 1 (c)), to a pulse signal (Figure 1 (d)).

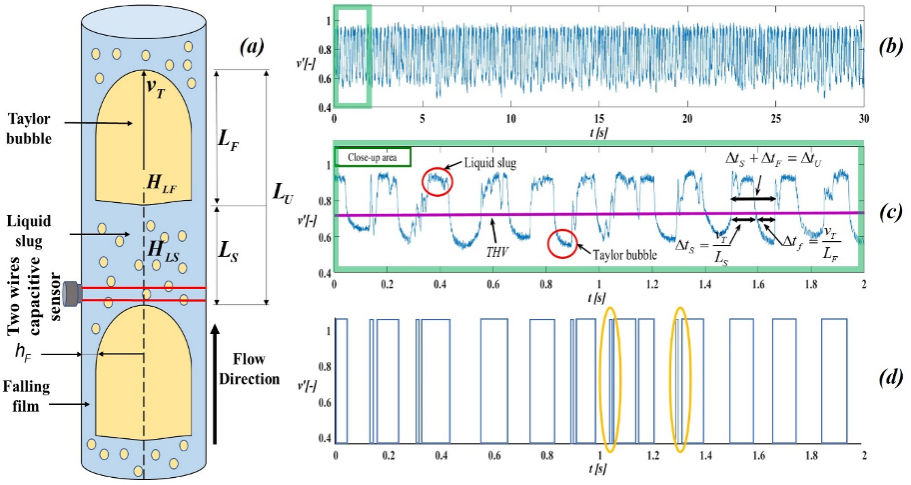

Fig. 1. Scheme of upward slug flow, using as an example the experimental test with $v_{SL} = 0.7$ ms^{-1}, $v_{SG} = 0.7$ ms^{-1}, and 85º of inclination angle (Soto-Cortes *et al*., 2019). a) Schematic diagram of the slug flow, b) normalized voltage signal from a capacitive filament sensor, c) approach to the normalized signal with the components of the slug flow and threshold cut, d) Pulses generated from the optimization proposed by Kouba (1986).

This value divides the signal into two sections called film and slug. For an instant of time t_i, if $THV<V'_{t_i}$, then $V'_{t_i}=1$. Otherwise $V'_{t_i}=0$. However, the resulting discrete signal (Figure 1 (d)) has some errors, as it includes some pulses that, due to their duration, cannot be considered as a slug. This is due to the presence of gas bubbles trapped in the liquid phase. Figure 1(d) shows in a yellow ovals an example of these errors.

Later Al-Safran, (2003) proposed an improvement to the method of Kouba (1986). He suggested two cutoff thresholds: one for the slug (THV_S) and another for the film (THV_F). Figure 2(a) illustrated the idea of these thresholds (green and red lines, respectively). In this case, the selection of the thresholds was made visually. The objective of the method was to double-check the valleys present in the voltage-time series and avoid unduly dividing the slug pulse. For an instant of time t_i; if $V'_{t_i}<THV_S$, but $V_{t_i}>THV_F$, then $V'_{t_i}=1$. Otherwise $V'_{t_i}=0$. The foregoing, as seen in Figure 2(b), compared to Figure 1(d), significantly reduces the number of wrong pulses (yellow ovals) for the same signal.

Brito (2012) investigated the impact of the determination of cutoff thresholds. She concluded that subjectivity in the selection of these requires a methodology that allows its determination automatically. Soto-Cortes (2014) proposed to eliminate this subjectivity through a method that divides the normalized time series into two regions: film and slug. This was done based on the histogram of frequencies of the electrical signal, under the hypothesis that each of the parts corresponds to a normal probability distribution function. This method discriminates the voltage values found in the transition between the film and slug zones. This methodology has been tested with good results (Soedarmo *et al*., 2018; Soto-Cortes *et al*., 2019) and is resumed in this work to propose a possible optimization from applying a second adjustment of the cut thresholds.

2 Materials and methods

2.1 *Probabilistic determination of cutting thresholds*

Soto-Cortes (2014) proposed to divide the histogram of electric frequencies into two regions: the slug and the film (Figure 3 (a)) and analyze them separately. He adjusted a non-parametric probabilistic distribution function (NP-PDF) and a normal distribution (Normal PDF) (Figures 3 (b) and (c)). These functions fit a sample with n observed data $x_i(i \in [1,n])$. For the NP-PDF, a smoothed random sampling was applied, while, in the case of the Normal PDF, it was characterized by the mean and the standard deviation.

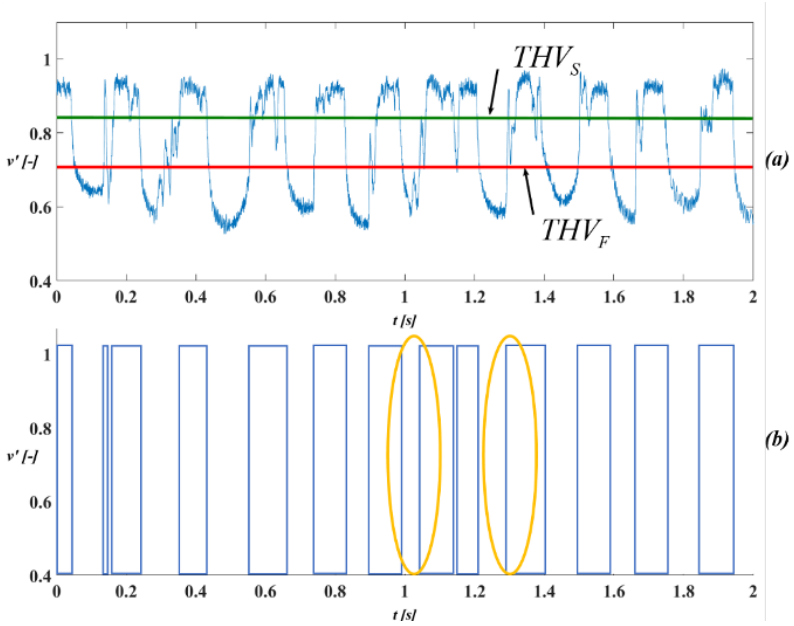

Fig. 2. Example of the optimization proposed by Al-Safran, (2003): a) application of the THV_S and THV_F cut-off thresholds visually defined to a normalized signal, b) transformation of the normalized signal to a pulse signal.

This hypothesis assumes that the adjustment of the normal distribution will improve when removing the right tail of the film region and the left tail of the slug region, which corresponds to the film - slug transition zone. To determine the cutoff threshold, Soto-Cortes (2014), compared the survival functions (Eq. 1), for the NP-PDF and the Normal PDF (Figure 3 (d) and (e)), through from the following equation:

$$S(V') = P(x > V') = 1 - F(V'), \qquad (1)$$

where S is the survival function, which depends on the normalized voltage (V') obtained from the distribution function F, adjusted to the population. The function S represents the probability that the observed value of x is higher than the value V'. From this comparison, Soto-Cortes (2014) proposed that film and slug cut thresholds correspond to the intersection between the survival functions of NP-PDF distributions and Normal PDF. He found that the thresholds are close to 75 and 25 percentile, respectively: $THV_{F(75)}$ and $THV_{S(25)}$. This methodology has been tested with good results (Soedarmo *et al*., 2018; Soto-Cortes *et al*., 2019).

2.2 *Recursive method application*

The methodology for the probabilistic determination of the cutoff thresholds proposed by Soto-Cortes (2014), has the hypothesis that the experimental data describing the slug and film regions conform to a normal distribution. If this is correct, after the application of the $THV_{F(75)}$ and $THV_{S(25)}$ cutoff thresholds, the resulting histograms should better fit to the distribution function. Therefore, in this study, it was decided to evaluate the effect of performing a second iteration of the procedure proposed by Soto-Cortes (2014), and check if there is an improvement in the determination of the regions from the new cutoff thresholds named THV_F* and THV_S* (Figure 4).

2.3 *Evaluation of the proposed methodology*

2.3.1 *Experimental database*

To test the performance of the proposed optimization methodology, used a set of 40 experimental data of upward slug flow in inclined tubes (45º, 60º, 70º, 80º, and 85º). The database included normalized voltage time series (acquisition frequency 1000 Hz). Soto-Cortes *et al*. (2019) described details of the installation and experimental campaign. They used mineral oil (Lubsoil ND 50-ISO 220, μ_L=213 mPa.s, ρ_L=873 kg m^{-3}, v_{SL} [0.05,0.7]m s^{-1}) and air (μ_G=0.2 mPa.s 35 ºC, μ_{SG} [0.5,6.0]m s^{-1}).

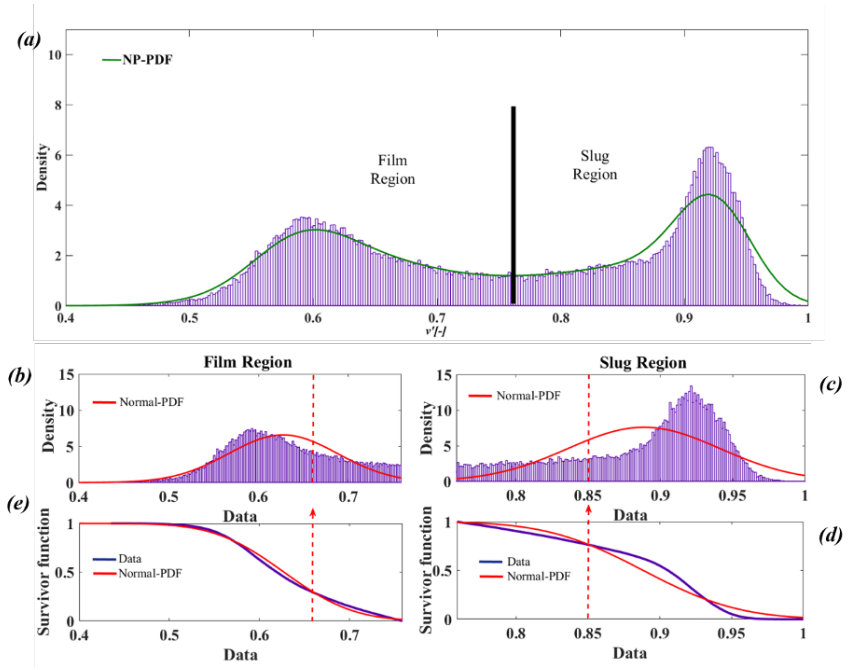

Fig. 3. Methodology for the determination of cut-off thresholds proposed by Soto-Cortes (2014): a) histogram of the typical normalized voltage signal from a slug flow, b) and c) histograms of the film and slug regions, respectively, and the adjustment from a Normal PDF, d) and e) comparison among survival functions for NP-PDF and Normal PDF, for the film and slug regions respectively. In the latter, the dashed red line illustrates the values of $THV_{F(75)}$ and THVS (25).

2.3.2 *Classification of the frequency histograms present in the database*

To evaluate the performance of the proposed optimization methodology, we classified the frequency histograms of the experimental tests into three categories: 2P-A (Figure 5 (a)), which corresponds to a typical slug flow distribution characterized by being bimodal with two peaks separated by a valley. The top left represents the film region and the right of the slug region. The time series it comes from shows small gas bubbles trapped in the slug body and clearly defined valleys, it translates into a slug region with a higher density than the film. Otherwise, it is the category called 2P-B (Figure 5 (b)), which appears at experimental points close to the transition between slug and churn flows (v_{SG}> 1 m s^{-1} and 0.05 > v_{SL} > 0.3 m s^{-1}). The entrapment of gas bubbles in the slug body generates a denser film region. Finally, the category called 3P (Figure 5 (c)) corresponds to a histogram which shows three modes: two in the film region and one in the slug region. It is presented with low gas velocities (v_{SG} ≤0.7 m s^{-1} and 0.05 > v_{SL} > 0.3 m s^{-1}). This behavior differs from 2P-A&B categories due to the third mode, in contrast to the ingrained idea that this flow pattern is bimodal (Kouba, 1986). In these terms, the 3P category is qualified as atypical just for classification purposes. The third mode, present in the high presence of liquid, corresponding to a time series with a pronounced plateau at the valley before a pronounced minimum. This because in the stratified region, the downward liquid flow obeys basically to gravity forces. Its velocity (film velocity), is calculated as v_F=v_T − v_{LF}. Based on a free surface flow condition, v_{LF} changes its value along the film length L_F, with a minimum at the end of the film, ahead of the following slug. This causes a backwater responsible of the third peak in the frequency histogram.

2.4 *Performance evaluation*

The methodology for the probabilistic determination of the cutoff thresholds by Soto-Cortes, (2014), and the optimization proposed in this work, were integrated into a MATLAB^{TM} code. The code automatically calculates the cutoff values, applies them to the time series, and obtains the discretized signal (pulses).

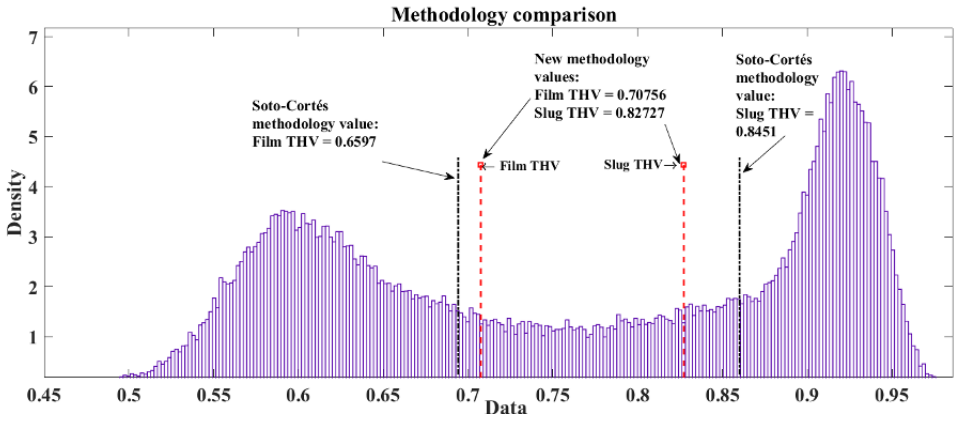

Fig. 4. Black lines show the cutoff thresholds determined by the methodology proposed by Soto-Cortes (2014); meanwhile, red lines show the thresholds established by the proposed optimization.

From the latter, calculate the number of slugs (S_n), and considering the duration of the signal (t_{TS}), estimate its frequency ($f_{slug,E}$) by Eq. 2.

$$f_{slug,E} = \frac{S_n}{t_{TS}} \tag{2}$$

From the available database (Soto-Cortés, 2014), we selected 40 representative cases. To verify the goodness of the results obtained, we analyzed their level of confidence. It was achieved from a manual count ($f_{slug,R}$) of the pulses of the signal for each selected experimental case. To provide further certainty in determining the level of confidence and reducing subjectivity, we made a repeatability exercise. It consisted of counting more than 30 times for each selected test.

Table 1. Selected tests for the repeatability exercise, according to the proposed classification.

Classification	Angle	v_{SL} (m/s)	v_{SG} (m/s)
2P-A	80	0.05	0.5
2P-A	45	0.5	0.5
2P-B	80	0.5	1.0
2P-B	45	0.1	1.0
3P	80	0.1	0.7
3P	45	0.05	0.7

The selected experiments are listed in Table 1, and these tests were chosen mainly by the classification described in Figure 5 (a, b, c), as well as the angle of inclination.

Table 2 presented the comparison between the confidence level from the visual count ($f_{slug,R}$), and the experimental uncertainty for the experimental methodologies ($f_{slug,E}$). In this way, the results show agreement for frequencies bigger than 50 pulses. It shows the number of tests (n), the frequency range (the number of pulses peaks counted), the level of confidence for 95%, and the uncertainty of the experimental test. The latter obtained by statistical analysis of the counts per test, and the average value of the uncertainties.

Since the uncertainty is the error associated with the measurement, having an approximate value to this implies having a parameter that allows giving certainty to the results.

To evaluate the performance of these methodologies, used six statistical parameters based on the current error (ε_a), and relative (ε_r) of the bump frequency f_{slug} Eq. (3) and Eq. (4), respectively,

Table 2. Comparison of the level of confidence of the visual count against uncertainty calculated during the application of the proposed optimization.

n	Frequency range	Confidence level	Uncertainty
3	<50	0.5888	1.8006
6	50-100	1.3069	1.5239
21	>100	5.3284	5.3454

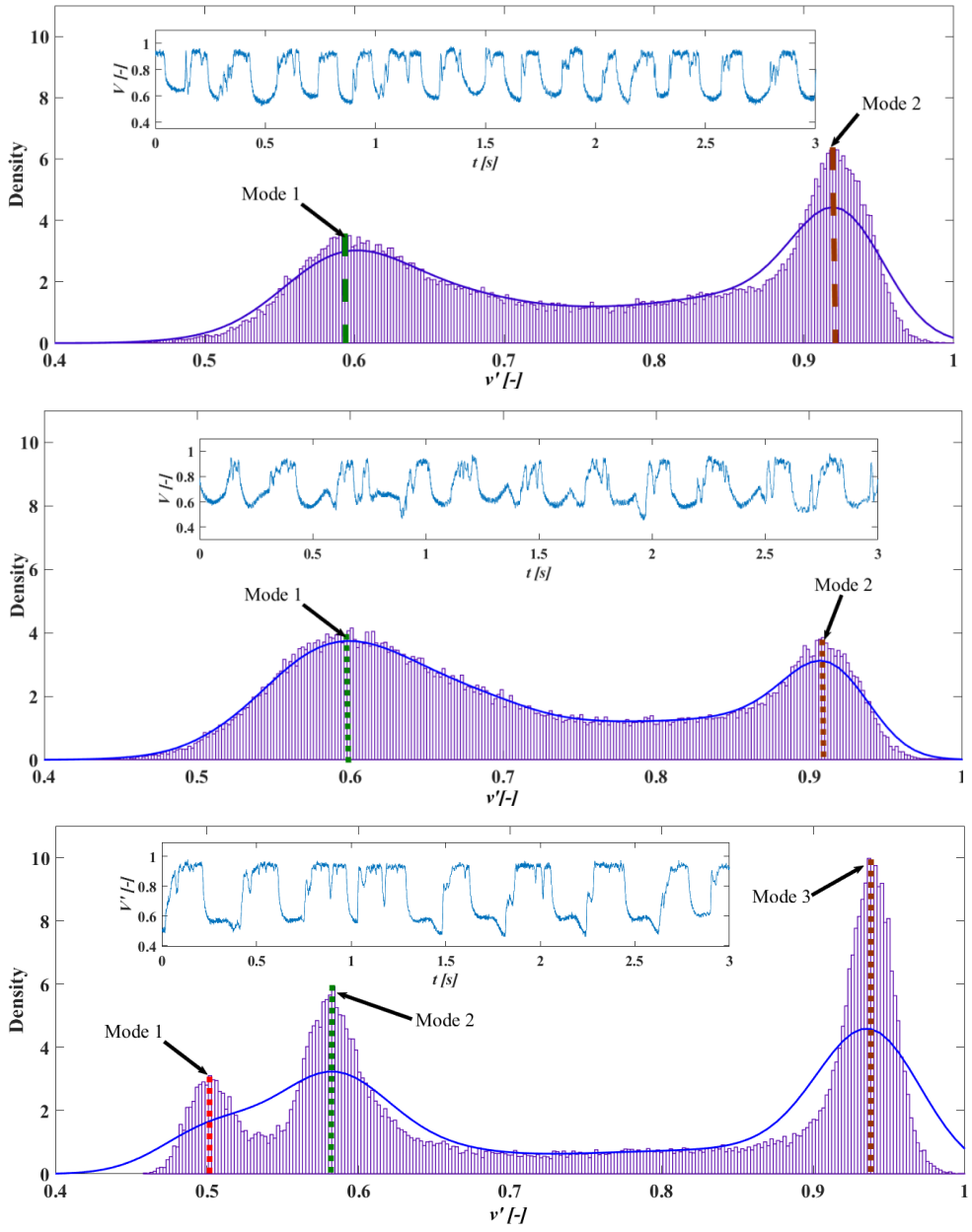

Fig. 5. Examples of the frequency histogram for slug flow pattern from the experimental information reported by Soto-Cortes *et al*., (2019), for an inclination angle of 85º: (a) v_{SL} = 0.7, v_{SG} = 0.7 m/s,, typical distribution of the slug flow, (b) v_{SL} = 0.5, v_{SG} = 1.0 m/s, distribution close to the slug-churn transition, (c) v_{SL} = 0.3, v_{SG} = 0.5 m/s, atypical distribution with three modes.

$$\varepsilon_a = f_{slug,E} - f_{slug,R} \tag{3}$$

$$\varepsilon_r = \frac{\varepsilon_a}{f_{slug,R}} 100 \tag{4}$$

The mean deviation, absolute and standard of the relative error are described in Eqs. (5-7) respectively,

$$e_1 = \frac{1}{N} \sum_{i=0}^{N} \varepsilon_{r_i} \tag{5}$$

$$e_2 = \frac{1}{N}\sum_{i=0}^{N}\left|\varepsilon_{r_i}\right| \tag{6}$$

$$e_3 = \sqrt{\frac{\sum_{i=0}^{N}(\varepsilon_{r_i} - e_1)^2}{N-1}} \tag{7}$$

3 Results and discussion

3.1 Evaluation of the optimization proposed

Figure 6 compares the values $f_{slug,R}$ from manual frequency counting versus $f_{slug,E}$ determined by the original method (red diamonds) by Soto-Cortes (2014), and the proposed optimization (blue squares).

It is observed that there is more dispersion of the results obtained by the proposed optimization, than those calculated by Soto-Cortes. To find an explanation, we used an analysis of the mean deviation of the relative error, which is an indication of the overestimation (+) or underestimation (-) at the time of the pulse count.

In Figure 7(A) the relative errors (Eqs. 5-7) for the 40 cases studied were grouped compared by the angle of inclination and by all tests analyzed. The proposed optimization (filled blue bars) found to overestimate the number of slug pulses for the inclination angles of 45°, 60°, and 70°. However, it shows favorable results for experimental tests performed with the angles of 80° and 85°, precisely the case when the highest slug frequencies are presented. When analyzing the mean deviation of the relative error by the type of classification, it found that the proposed optimization performs a better behavior for the tests within the 3P classification, which represent the most complex case due to the geometry of the signal Figure 7 (B).

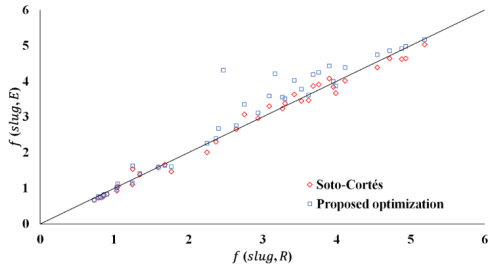

Fig. 6. Comparison of manual counting $f_{slug,R}$ versus experimental methodologies $f_{slug,E}$, in red diamonds by Soto-Cortes (2014) and blue squares by the proposed optimization.

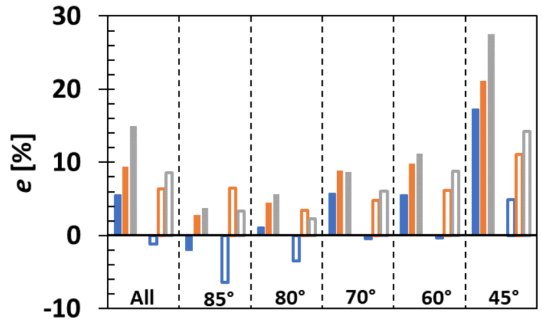

(a)

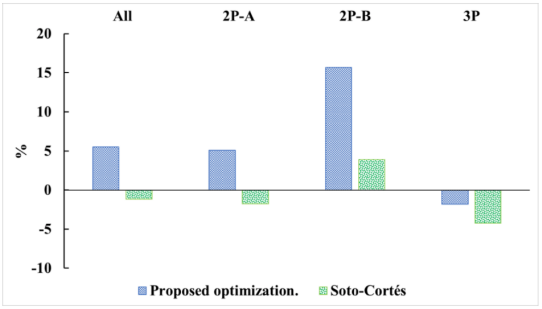

(b)

Colors: e_1 e_2 e_3
Optimization (filled bars) – Soto-Cortes (unfilled bars)

Fig. 7. Calculated errors for the analysis of results between the proposed optimization (filled bars) and the Soto-Cortés methodology (unfilled bars). (A) relative error comparison by inclination angle, (B) the mean deviation of the relative error by the type of classification.

Conclusions

By applying a second adjustment to the probability functions to determine the cutoff thresholds to define the film and slug regions, we obtain the following findings. In general, the proposed optimization overestimated the slug numbers compared to those obtained with the Soto-Cortes (2014) methodology. However, when comparing the average deviation of the relative error of each methodology, it found that the proposed optimization has better results when the flow is close to the vertical (Figure 7a). With an inclination angle of 80° e_1 is around 1% for the optimized procedure, against -3% for the original methodology. For the angle of 85°, these relative errors become -2% and -6%, respectively.

Also, when comparing the average error deviation calculated by the type of classification defined, it found that the proposed optimization presents better results for the 3P classification (Figure 7b). This is around -2% for the optimized procedure against -4% in the original methodology. This, despite the complexity of this kind of signal.

Although the procedure for selecting and determining the cutoff thresholds for each section eliminated the subjectivity, the results obtained indicate that a second adjustment is only recommended for pipes near the vertical. Therefore, in general, the recommendation should be to use a combination of the methodology proposed here for angles higher than 80° and the methodology by Soto-Cortes for smaller than 80°.

Acknowledgements

The authors would like to acknowledge: (A) the members of the Tulsa University Fluid Flow Project (TUFFP) for their support of this research program. (B) To the Mexican Council of Science and Technology, Mexico (CONACyT, 2013, request 207653). (C) To the National Supercomputing Laboratory of Southeast Mexico, CONACYT member of the network of national laboratories, Project: 201903068N. (D) - To the Secretary of Public Education, Subsecretariat of Higher Education, for supporting project 30509 - Strengthening of Academic Bodies PRODEP.

Nomenclature

Nomenclature

CH	Churn flow
f	Frequency
h	Thickness
H_L	Holdup
L	Length
S_n	Number of slugs
SL	Slug flow
t_{TS}	Test duration
THV	Threshold value
v	Velocity m.s^{-1}
V'	Normalized voltage
$3P$	Classification type

Greek letters

μ	Viscosity kPa.s
ρ	Density kg.m^{-3}
θ	Inclination angle

Subscripts

a	Actual
E	Experimental
F	Film
g	Gas phase
L	Liquid phase
r	relative
R	Real
S	Slug
t	Total
U	Cycle

References

Al-Kayiem, H. H., Mohmmed, A. O., Al-Hashimy, Z. I., and Time, R. W. (2017). Statistical assessment of experimental observation on the slug body length and slug translational velocity in a horizontal pipe. *International Journal of Heat and Mass Transfer 105*, 252-260. https://doi.org/10.1016/j.ijheatmasstransfer.2016.09.105

Al-Ruhaimani, F., Pereyra, E., Sarica, C., Al-Safran, E., Chung, S., and Torres, C. (2018). A study on the effect of high liquid viscosity on slug flow characteristics in upward vertical flow. *Journal of Petroleum Science and Engineering 161*, 128-146. https://doi.org/10.1016/j.petrol.2017.11.047

Al-Safran, E. M. (2003). *An Experimental and Theoretical Investigation of Slug Flow Characteristics in the Valley of a Hilly*., Ph.D. Dissertation, 186 Pp, The University of Tulsa, OK, USA.

Al-Safran, E. M. (2016). Probabilistic modeling of slug frequency in gas/liquid pipe flow using the Poisson probability theory. *Journal of Petroleum Science and Engineering 138*, 88-96. https://doi.org/10.1016/j.petrol.2015.12.008

Alboudwarej, H., Felix, J., Taylor, S., Badry, R., Bremner, C., Brough, B., and West, C. (2006). Heavy oil. *Oilfield Review 18*, 34-53. https://doi.org/http://dx.doi.org/10.1017/S1479262113000075

Al-Ruhaimani, F. A. S. (2015). *Experimental analysis and theoretical modeling of high liquid viscosity two-phase upward vertical pipe flow.* Ph.D. Dissertation, 318 Pp, The University of Tulsa, Ok, USA

Archibong-Eso, A., Baba, Y., Aliyu, A., Zhao, Y., Yan, W., and Yeung, H. (2018). On slug frequency in concurrent high viscosity liquid and gas flow. *Journal of Petroleum Science and Engineering 163*, 600-610. https://doi.org/10.1016/j.petrol.2017.12.071

Álvarez del Castillo, A., Santoyo, E., García-Valladares, O., & Sánchez-Upton, P. (2010). Evaluación estadística de correlaciones de fracción volumétrica de vapor para la modelación numérica de flujo bifásico en pozos geotérmicos. *Revista Mexicana de Ingeniería Química 9*, 285-311.

Baba, Y. D., Aliyu, A. M., Archibong, A.-E., Almabrok, A. A., and Igbafe, A. I. (2017a). Study of high viscous multiphase phase flow in a horizontal pipe. *Heat and Mass Transfer*. https://doi.org/10.1007/s00231-017-2158-5

Baba, Y. D., Aliyu, A. M., Archibong, A. E., Abdulkadir, M., Lao, L., and Yeung, H. (2018). Slug length for high viscosity oil-gas flow in horizontal pipes: Experiments and prediction. *Journal of Petroleum Science and Engineering 165*, 397-411. https://doi.org/10.1016/j.petrol.2018.02.003

Baba, Y. D., Archibong, A. E., Aliyu, A. M., and Ameen, A. I. (2017b). Slug frequency in high viscosity oil-gas two-phase flow: Experiment and prediction. *Flow Measurement and Instrumentation 54*, 109-123. https://doi.org/10.1016/j.flowmeasinst.2017.01.002

Brito, R., (2012). *Effect of medium oil viscosity on two-phase oil-gas flow behavior in horizontal pipes*. Masters Degree Dissertation, 285 Pp, The University of Tulsa, USA.

Brito, R., Pereyra, E., and Sarica, C. (2014). Experimental study to characterize slug flow for medium oil viscosities in horizontal pipes. *9th North American Conference on multiphase technology*, Banf, Canada, 15Pp. https://www.onepetro.org/conference-paper/BHR-2014-G4

Chung, S., Pereyra, E., Sarica, C., Soto, G., Alruhaimani, F., and Kang, J. (2016). Effect of high oil viscosity on oil-gas flow behavior in vertical downward pipes. B*HR Group - 10th North American Conference on Multiphase Technology 2016*, 259-270. https://doi.org/10.1016/j.expthermflusci.2019.109896

Davies, R. M., and Taylor, G. (1950). The mechanics of large bubbles rising through extended liquids and through liquids in tubes. *Proceedings of the Royal Society A: Mathematical, Physical and Engineering Sciences 200*, 375-390. https://doi.org/10.1098/rspa.1950.0023

Sánchez-Silva, F., Carvajal-Mariscal, I., Rejón-Torres, R., and Toledo-Velázquez, M. (2018). Experimental study of the biphasic flow behavior at low superficial velocities in an inclined-vertical pipe combination. *Revista Mexicana de Ingeniería Química 17*, 303-316. https://doi.org/10.24275/uam/izt/dcbi/revmexingquim/2018v17n1/Sanchez

Gfeller, F. R., and Bapst, U. (1979). Wireless in-house data communication via diffuse infrared radiation. *Proceedings of the IEEE 67*, 1474-1486. https://doi.org/10.1109/PROC.1979.11508

Gonçalves, G. F. N., Baungartner, R., Loureiro, J. B. R., & Silva Freire, A. P. (2018). Slug flow models: Feasible domain and sensitivity to input distributions. *Journal of Petroleum Science and Engineering 169*, 705-724. https://doi.org/10.1016/j.petrol.2018.05.008

Gregory, G. A., Nicholson, M. K., & Aziz, K. (1978). Correlation of the liquid volume fraction in the slug for horizontal gas-liquid slug flow. *International Journal of Multiphase Flow 4*, 33-39. https://doi.org/10.1016/0301-9322(78)90023-X

Jaeger, J., Santos, C. M., Rosa, L. M., Meier, H. F., & Noriler, D. (2018). Experimental and numerical evaluation of slugs in a vertical air-water flow. *International Journal of Multiphase Flow 101*, 152-166. https://doi.org/10.1016/j.ijmultiphaseflow.2018.01.009

Kouba, G. E., (1986). *Horizontal Slug Flow Modeling and Metering*. Ph.D. Dissertation, 155 P, University of Tulsa, Ok, USA.

Losi, G., Arnone, D., Correra, S., & Poesio, P. (2016). Modeling and statistical analysis of high viscosity oil/air slug flow characteristics in a small diameter horizontal pipe. *Chemical Engineering Science 148*, 190-202. https://doi.org/10.1016/j.ces.2016.04.005

Saidj, F., Hasan, A., Bouyahiaoui, H., Zeghloul, A., & Azzi, A. (2018). Experimental study of the characteristics of an upward two-phase slug flow in a vertical pipe. *Progress in Nuclear Energy 108*, 428-437. https://doi.org/10.1016/j.pnucene.2018.07.001

Salazar-Mendoza, R., García-Gutiérrez, A., & Aragón-Jerónimo, A. (2004). A two-region averaging model for solid-liquid flow with a moving bed in horizontal pipes. *Revista Mexicana de Ingeniería Química 3*, 273-286.

Shoham, O. (2005). *Mechanistic Modeling of Gas Liquid Two Phase Flow in Pipes*. Society of Petroleum Engineers, 310p, USA.

Soedarmo, A., Soto-Cortes, G., Pereyra, E., Karami, H., & Sarica, C. (2018). Analogous behavior of pseudo-slug and churn flows in high viscosity liquid system and upward inclined pipes. *International Journal of Multiphase Flow 103*, 61-77. https://doi.org/10.1016/j.ijmultiphaseflow.2018.02.001

Soto-Cortes, G. (2014). *Effects of High Oil Viscosity on Oil-Gas Behavior in Deviated Pipes*. Pp. 211-23 in TUFFP 83rd Semi-Annual Advisory Board Meeting, edited by TUFFP. Tulsa, OK: University of Tulsa. Retrieved November 21, 2019 (https://www.scopus.com/record/display.uri?eid=2-s2.0-85045122538&origin=inward).

Soto-Cortes, G., Pereyra, E., Sarica, C., Rivera-Trejo, F., & Torres, C. (2019). Effects of high oil viscosity on oil-gas upward flow behavior in deviated pipes. *Experimental Thermal and Fluid Science 109*, 109896. https://doi.org/10.1016/j.expthermflusci.2019.109896

Taitel, Y., and Barnea, D. (1990). Two-phase slug flow. *Advances in Heat Transfer 20*, 83-132. https://doi.org/10.1016/S0065-2717(08)70026-1

Taitel, Y., and Dukler, A. E. (1977). A model for slug frequency during gas-liquid flow in horizontal and near horizontal pipes. *International Journal of Multiphase Flow 3*, 585-596. https://doi.org/10.1016/0301-9322(77)90031-3

Thaker, J., and Banerjee, J. (2015). Characterization of two-phase slug flow sub-regimes using flow visualization. *Journal of Petroleum Science and Engineering 135*, 561-576. https://doi.org/10.1016/j.petrol.2015.10.018

Thaker, J., and Banerjee, J. (2016). On intermittent flow characteristics of gas-liquid two-phase flow. *Nuclear Engineering and Design 310*, 363-377. https://doi.org/10.1016/j.nucengdes.2016.10.020

Wu, B., Firouzi, M., Mitchell, T., Rufford, T. E., Leonardi, C., & Towler, B. (2017). A critical review of flow maps for gas-liquid flows in vertical pipes and annuli. *Chemical Engineering Journal 326*, 350-377. https://doi.org/10.1016/j.cej.2017.05.135

Zhang, M., Pan, L. ming, He, H., Yang, X., & Ishii, M. (2018). Experimental study of vertical co-current slug flow in terms of flow regime transition in relatively small diameter tubes. *International Journal of Multiphase Flow 108*, 140-155. https://doi.org/10.1016/j.ijmultiphaseflow.2018.07.005